

In-Situ Stress-Strain Measurements of Bridgmanite at the Lower Mantle Pressure Conditions

We conducted in-situ stress-strain measurements of bridgmanite using the deformation-111 type apparatus to determine the viscosity of bridgmanite at the uppermost lower mantle conditions in the dislocation creep region. The viscosity of bridgmanite would be harder than those of olivine and its polymorphs under nominally dry conditions, which is consistent with the geophysical observation. Grain-size and stress conditions of bridgmanite at the top of the lower mantle are expected by deformation mechanism maps and geophysical observations of several millimeters and $\sim 10^5$ Pa. This grain-size suggests that the main part of the lower mantle is isolated from mantle convection as primordial reservoirs

Rheological properties, including the viscosity of the constituent mantle minerals, are fundamental to understanding the dynamics of the Earth's mantle. The Earth's mantle consists of upper mantle (>410 km depth), transition zone (410 km to 660 km depth), and lower mantle (660 km to 2900 km depth), which have been distinguished by seismic and mineralogical studies. The lower mantle occupies ~ 65 vol.% of Earth's mantle. One-dimensional viscosity-depth models of Earth's mantle proposed from geophysical observations [e.g., 1] indicate that the lower mantle is the most viscous of all mantle layers, with a viscosity of 10^{19-21} Pa·s. In addition, viscosities contrast between the transition zone and that of the top of the lower mantle have been assessed 1-2 orders of magnitude. Bridgmanite, which

is (Mg,Fe)SiO₃-perovskite with space group Pbnm, is the most abundant mineral in the Earth's lower mantle. Therefore, it is important for understanding the Earth's mantle dynamics to know the viscosity of bridgmanite.

In the Earth's mantle, dominant deformation mechanisms are generally considered to be diffusion creep and/or dislocation creep. The total strain (ϵ_{total}) during deformation is the sum of the strains of diffusion creep (ϵ_{dif}) and dislocation creep (ϵ_{dis}), and viscosity (η) is defined as $\eta = \sigma / \dot{\epsilon}_{total}$ where σ and $\dot{\epsilon}_{total}$ are stress and total strain rate, respectively. Diffusion creep of bridgmanite has been studied mainly by diffusion experiments under deep mantle conditions [e.g., 2], whereas dislocation creep of bridgmanite is still unclear because of experimental difficulties. In order to determine the

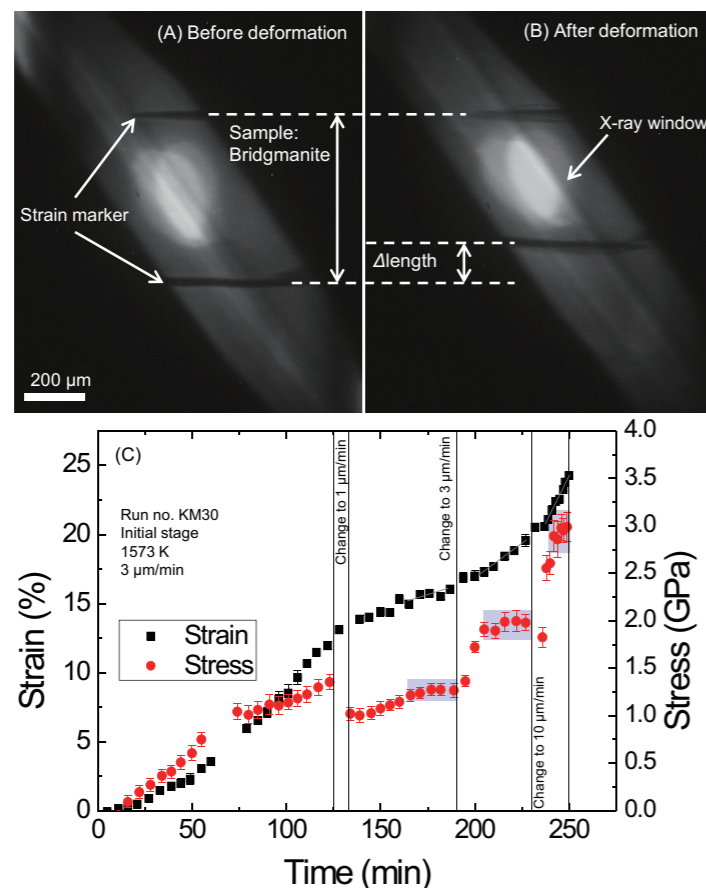


Figure 1: X-ray radiographs of bridgmanite deformation experiments in run KM30 (A) before deformation and (B) after deformation. (C) Time evolution of stress and strain of bridgmanite aggregate in run KM30.

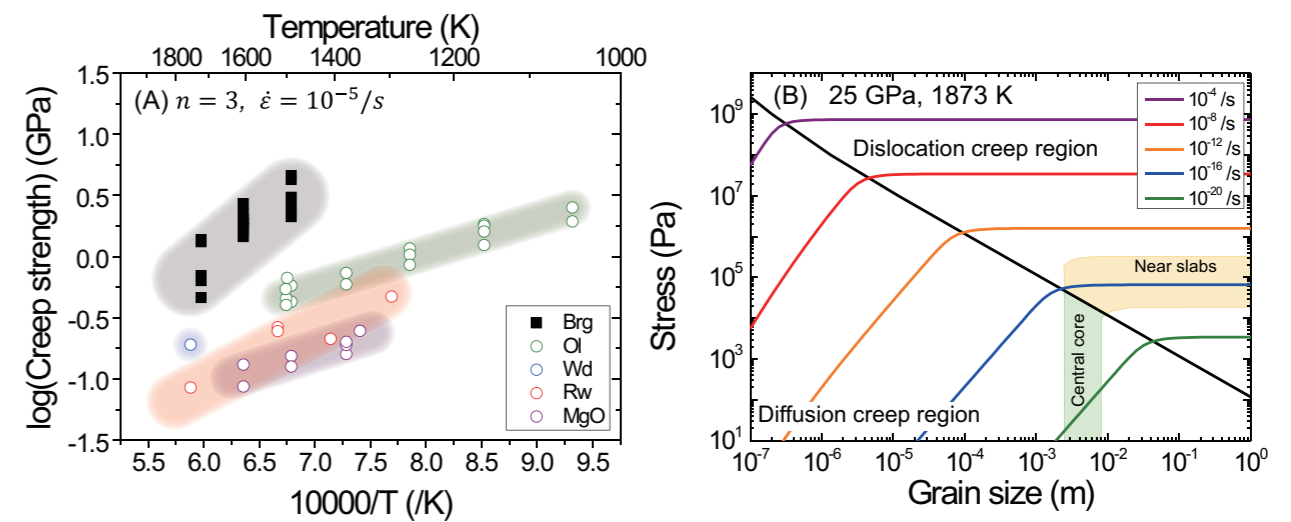


Figure 2: (A) Comparison of creep strength of bridgmanite with those of olivine and its polymorphs normalized at strain rate $\dot{\epsilon}$ of $10^{-5}/s$ with stress exponent n of 3. (B) Deformation mechanism map of bridgmanite at 25 GPa and 1873 K.

viscosity of bridgmanite in the dislocation creep region, in-situ stress and strain measurements of MgSiO₃ bridgmanite during uniaxial deformation at temperatures of 1473-1673 K and pressures of 23-27 GPa were conducted by using the Kawai-type cell assembly with the deformation-111 type apparatus AR-NE7A [3]. The maximum strain of bridgmanite reached ~ 30 % as shown in Fig. 1(A) and (B). The large strain obtained by the deformation-111 type apparatus enables us to realize in-situ measurements of several steady-state creep conditions in each experiment as shown in Fig. 1(C). Stress and strain-rate in the deformation experiments encompassed from 0.9 to 4.5 GPa and from 4.9×10^{-6} to $1.5 \times 10^{-4} s^{-1}$, respectively.

Figure 2(A) represents the creep strengths in the dislocation creep of bridgmanite and other mantle minerals. These creep strength data were obtained under nominally dry conditions, although ringwoodite and wadsleyite, which are olivine's polymorphs at the mantle transition zone, are with a small amount of water (0.029-0.1 wt.%). The creep strength of bridgmanite is higher than those of olivine and its high-pressure polymorphs, and periclase. In addition, Fig. 2(A) shows that the creep strength of bridgmanite is approximately one order of magnitude larger than that of ringwoodite. Therefore, the viscosity variation by geophysical observations between the mantle transition zone and the top of the lower mantle would be explained by the creep strength contrast between bridgmanite and ringwoodite in dislocation creep region even under nominally dry conditions.

The deformation mechanism map of bridgmanite at 1873 K and 25 GPa was constructed as shown in Fig. 2(B) based on the flow law of dislocation creep of bridgmanite [3] and diffusion coefficients reported by

annealing experiments [2] for diffusion creep. In order to realize a viscosity of 10^{21-22} Pa·s for the top of the lower mantle, stress magnitude and strain-rate are required to be 2×10^4 to 3×10^5 Pa in the grain-size insensitive dislocation creep regime respectively. These stress magnitudes of bridgmanite are consistent with those in the upper mantle estimated from the flow laws of olivine. Therefore, it is concluded that the rheology of the lower mantle is dominated by bridgmanite, which means that bridgmanite forms the load-bearing framework in the lower mantle rocks to control the lower mantle viscosity. In the stress-independent diffusion creep regime grain-size of 3–8 mm is demanded by deformation mechanisms maps whereas that of bridgmanite after phase transition from the transition zone is estimated to be less than several hundred micrometers even by 1 billion years [4]. This indicates that the lower mantle materials, which have viscosities comparable to the lower mantle, would not have experienced the phase transition during mantle convection. Therefore, the main portion of the lower mantle would have been isolated from mixing by mantle stirring and remained as ancient mantle.

REFERENCES

- [1] G. Soldati, L. Boschi, F. Deschamps and D. Giardini, *Phys. Earth Planet. Int.* **176**, 19 (2009).
- [2] D. Yamazaki, T. Kato, H. Yurimoto, E. Ohtani and M. Toriumi, *Phys. Earth Planet. Int.* **119**, 299 (2000).
- [3] N. Tsujino, D. Yamazaki, Y. Nishihara, T. Yoshino, Y. Higo and Y. Tange, *Sci. Adv.* **8**, eabm1821 (2022).
- [4] D. Yamazaki, T. Kato, E. Ohtani and M. Toriumi, *Science* **274**, 2052 (1996).

BEAMLINE
AR-NE7A

N. Tsujino^{1,2} (¹Okayama Univ., ²JASRI)